

Fabrication And Characterization Of CdO₂ Nanoparticles For Solar Cells Applications

¹Nadir F. Habubi, ²Muneer H. Jadduaa, ²Alaa Z.Ckal

¹College of Education, Al-Mustansiriyah University, Baghdad, Iraq.

² College of Science, Wasit University, Wasit, Iraq.

Corresponding author, E-mail: ahmed_naji_abd@yahoo.com

Abstract—In this study, CdO₂ thin films, which was prepared by chemical method and deposited by drop casting technique on glass and silicon substrates have been studied . The structural, optical and chemical analysis were investigated. X-ray diffraction (XRD) measurements reveal that the CdO₂ thin film was polycrystalline, cubic structure and there is no trace of the other material. UV-Vis measurements assure that the energy gap of CdO₂ thin film was found to be 2.5eV. I-V characterization of the solar cell under illumination at 40mW/cm² fluence was investigated . The open circuit voltage (V_{oc}) was 4.7V and short-circuit current density (I_{sc}) was 0.38 mA . These measurements show that the fill factor (FF) and the conversion efficiency (η) ,were 29.4% and 1.66% respectively.

Keywords—CdO₂, Thin film, XRD, Energy gap, Drop casting , Solar cells, AFM

1- Introduction

Cadmium oxide is transparent conducting oxides (TCOs) materials that hold both high electrical conductivity

2- Materials and Methodology

In a typical procedure, 1.5g of Cd(NO₃)₂.H₂O ,(BDH Chemicals Ltd Pool England) was dissolved in 50 ml of PVC (Sigma Aldrich USA) 1WT%. and ethanol (99.9%)was used throughout the experiment. The solution was put into a round-bottom flask with stirring. The color of the mixture was transparent. 25ml of NaOH (1M) was rapidly added to the mixture, and a nanopowder suspension was formed as shown in figure 1.The suspension was kept at 75°C for 1h. After cooling at room temperature, the particles were separated by centrifugation and were washed with ethanol to remove any contaminations.

and high optical transparency (>80%) in the visible light region of the electromagnetic spectrum [1]. CdO is a n-type semiconductor with nearly metallic conductivity [2]. It has a direct energy band gap (E_g) of ~2.3 eV and two indirect transitions at lower energies [3].CdO has extensive of applications as solar cells, windows, flat panel display, photo transistors.. It was experimentally proven that structural, electrical and optical properties are very sensitive to the film structure and deposition conditions [4,5]. Such transparent conductors are being used comprehensively in thin film solar cells [6] and optoelectronic devices [7].CdO films can be synthesized by many techniques such as sputtering [8], chemical vapor deposition (CVD) [9], spray pyrolysis [10], thermal evaporation [11] sol gel [12], and chemical bath deposition [13] Among various methods, spray pyrolysis is one through which the films can be coated for large area. In this work, the structural and optical properties of CdO₂ thin films deposited on glass and silicon wafer are prepared in order to estimate some physical properties of this metal oxides. According to our knowledge this is the first trial to examine the use of CdO₂ prepared by a simple chemical method for solar cell applications.



Fig. 1. CdO₂ freshly colloidal nanoparticles dissolved in PVC.

X-ray diffractometer (XRD-6000, Shimadzu) was used to investigate the structure and crystallinity of nanoparticles. The absorption of the colloidal nanoparticles solution was measured by using UV-Vis (UV -1800, Shimadzu, Japan)

3- Results and discussion

The XRD diffraction patterns of synthesized CdO₂ nanoparticles films prepared by quick chemical method were shown in Figure 2. Two peaks at $2\theta = 29.53^\circ$ and 48.04° corresponds to (111) and (220) planes were observed respectively ,which belong to CdO₂ cubic structure (JCPDS card no.039-1221), The crystallite size (D) was calculated by using Scheerer's formula [14].

$$D = \frac{0.94 \lambda}{\beta \cos \theta} \quad (1)$$

Where λ is the x-ray wavelength of CuK α source ($\lambda=0.154056$ nm), θ is the Bragg's angle and β is the full width at half maximum (FWHM) of the diffraction peak in radians. The dislocation density (δ) and microstrain (γ) values are calculated by using the following relations [15].

$$\delta = \frac{1}{D^2} \quad (2)$$

$$\gamma = \frac{\beta \cos(\theta)}{4} \quad (3)$$

The calculated grain size, microstrain and dislocation density values are presented in Table 1.

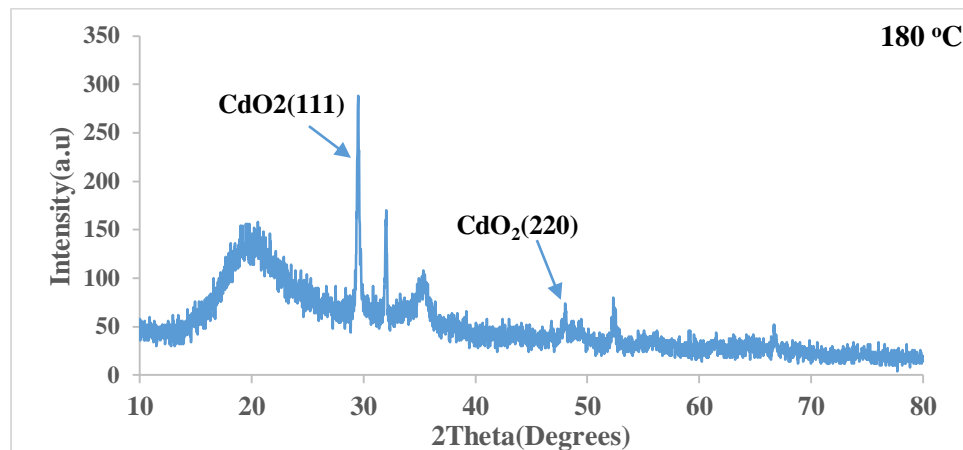


Fig. 2. XRD pattern of CdO₂ thin films ,which prepared by chemical method and deposited by drop casting technique on glass at Annealing temperature of 180 °C.

Table 1. X-Ray characterization for CdO₂ nanoparticles at 180 °C

2θ (deg)	(hkl) planes	β (deg)	D (nm)	$\delta \times 10^{14}$ lines.m ⁻²	$\gamma \times 10^{-4}$ Lines ⁻² .m ⁻⁴
29.53	CdO ₂ (111)	0.26	33.23	9.1	10.89
48.04	CdO ₂ (220)	0.2	45.4	4.9	7.97

The values of microstrain and dislocation density of CdO₂ nanostructure films prepared by chemical reaction were listed in Table 1.

Figure 3 shows 3D AFM image and Granularity accumulation distribution chart of CdO₂ nanoparticles

prepared by chemical method and deposited on glass substrate at 180°C. AFM images prove that the grains are uniformly distributed within the scanning area (4000×4000) nm with individual columnar grains extending upwards.

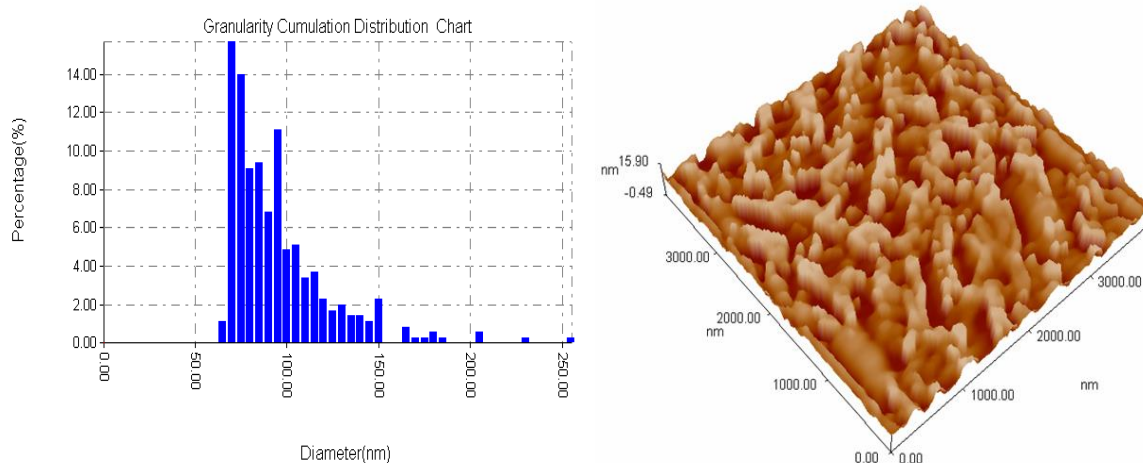


Fig. 3. 3D AFM images of CdO_2 thin film surface and Granularity accumulation distribution chart at Annealing 180°C .

The CdO_2 NPs have spherical shaped with good dispensability, homogeneous grains aligned vertically. The estimated values of root mean square (RMS) of surface roughness average and average grain size are listed in Table 2.

Table 2. Average diameter Size, Roughness and root mean square of CdO_2 NPs

Average Diameter Size (nm)	Roughness Density (nm)	Root Mean Square (nm)
93	2.23	2.59

Figure 4 shows the transmittance spectrum of CdO_2 thin film. The data are corrected for glass transmission in UV region. Also, the figure shows the transmission spectra increases with increasing the wavelength.

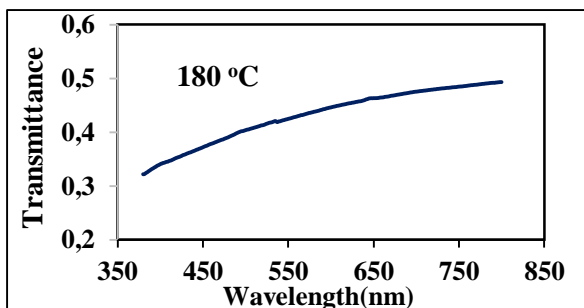


Fig. 4. Transmittance spectrum of CdO_2 thin films

The absorbance spectrum shown in Figure 5 . It was clearly seen that there was a sharp decrease in absorbance with decrease the wavelength.

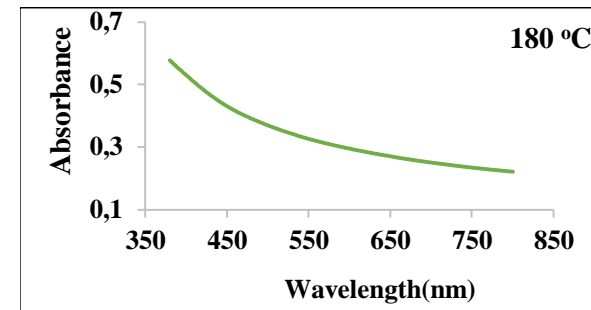


Fig. 5. Absorbance of the as deposited CdO_2 thin films

If T is the transmittance and A is the absorbance of the CdO_2 thin film. The reflectance of the film has been found by using relationship:

$$T+A+R=1 \quad (4)$$

The reflectance of the CdO_2 thin film increases with increasing the wavelength as shown in figure 6 due to increase in transmittance .

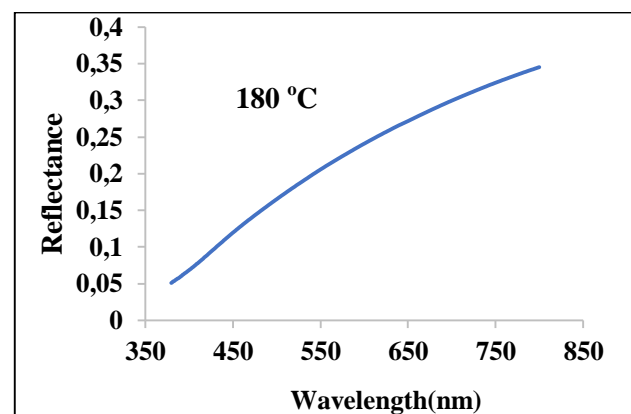


Fig. 6. Reflectance spectrum of CdO_2 thin films

The optical absorption coefficient α was evaluated by Tauc relation $\alpha h\nu = A(h\nu - E_g)^n$ Where $\alpha = 2.303 \frac{A}{t}$ and t is the film thickness, $h\nu$ is the photon energy, $E_g = \frac{1240}{\lambda(nm)}$ and $n = 0.5$ for direct allowed transition. Plotting the graph between $(\alpha h\nu)^2$ versus photon energy ($h\nu$) gives the value of

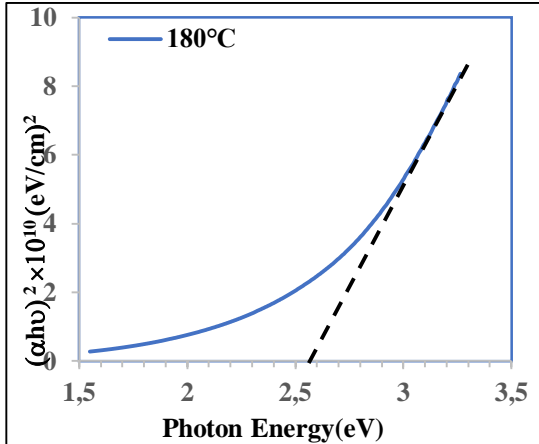


Fig.7: $(\alpha h\nu)^2$ versus photon energy plot of CdO_2 thin films

From the reflectance R of the thin film, the refractive index can be calculated from the following relationship[16]:

$$n = \frac{1+\sqrt{R}}{1-\sqrt{R}} \quad (5)$$

The refractive index (n) of the prepared CdO_2 films has been calculated using equation 5, for a range of wavelength of 380 nm to 800 nm. The plot of n versus wavelength was shown in Fig. 8. The refractive index of the film increases with increasing the wavelength.

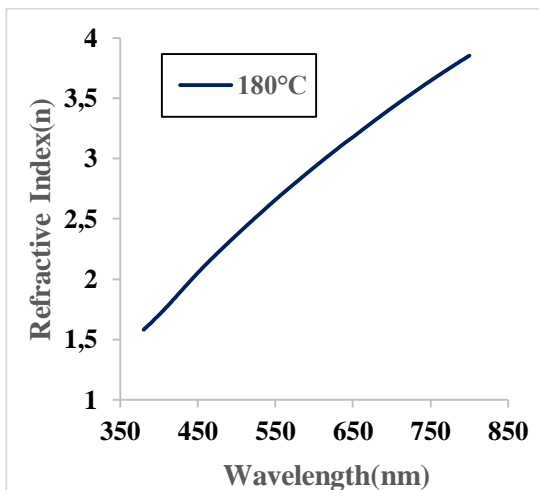


Fig.8: Refractive index spectrum of CdO_2 thin films

direct band gap. The extrapolation of the straight line to $(\alpha h\nu)^2 = 0$, gives the value of band gap, as shown in figure 7 the optical band gap was equal to 2.5 eV, in other word, the exciting wavelength ~ 496 nm . This result is very important to judge if this film can be used in a solar cell device.

Figure (9) shows the plot between photon energy versus extinction coefficient (k). The extinction coefficient with increases the photon energy. The dielectric constant and absorption coefficient are related and can be obtained theoretically with the relation given by the following: [Ugwu, 2006; Okujagu, 1992; P arachiniet et al., 1980; Chalkwski, 1980; Born et al., 1970; and Jenkins et al., 1976].

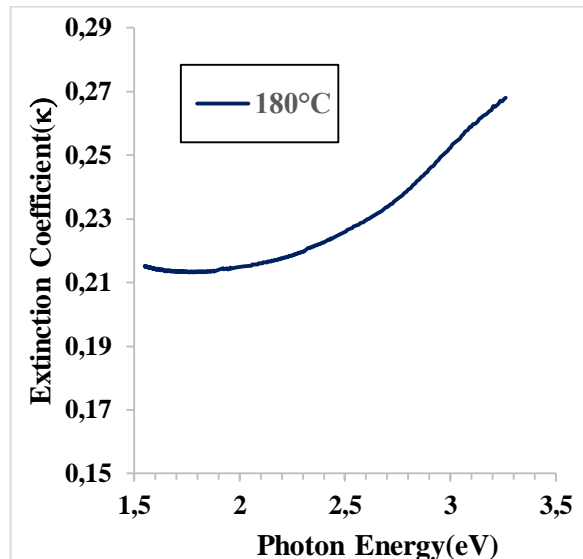


Fig. 9: extinction coefficient versus photon energy of CdO_2 thin film.

$$\varepsilon_r = n^2 - k^2 \quad (6)$$

$$\varepsilon_i = 2nk \quad (7)$$

. Where ε_r is the real part of the dielectric constant and ε_i is the imaginary part of the dielectric constant .The real part as shown in figure 10(a) almost decreases slowly with increasing photon energy .Also the figure indicates the absorption edge is the point which decreases the real part of the dielectric constant. The imaginary part of dielectric represents the absorption associated of radiation by free carriers and imaginary part is always positive and represented loss factor or energy absorbed. Also the figure 10(b) relieve that the imaginary part of CdO_2 thin film decreases with increases the photon energy.

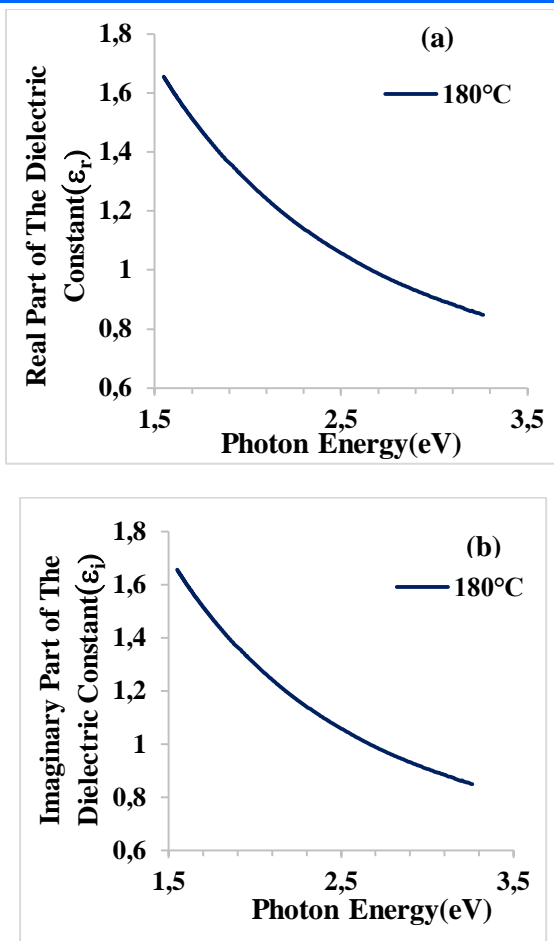


Fig.10: plot between photon energy with a: real part of the dielectric constant and b: the imaginary part of the dielectric constant

The imaginary part of dielectric constant is related to the optical conductivity (σ) which calculated from the following relation [17]:

$$\sigma = \alpha n c \epsilon_0 = \frac{\alpha n c}{4\pi} \quad (8)$$

Where σ is the optical conductance, c is the velocity of the radiation in the space, n is the refractive index and α is the absorption coefficient . Figure (11) shows the relation of optical conductivity with the incident photon energy. The increased optical conductivity at high photon energy is due to high absorbance of CdO₂ film in that region. The optical conductance and band gap indicated that the film is transmittance within the visible range, then it is suitable as a window in solar cell application

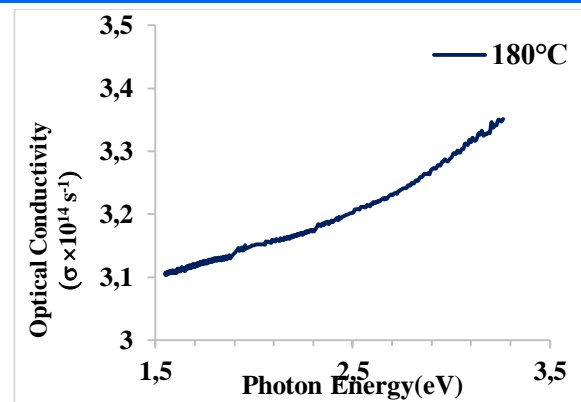


Fig.11: Optical conductivity of CdO₂ thin film as a function of photon energy

Figure 12 shows the I-V dark characteristics in forward and reverse direction of n-CdO₂/p-Si solar cell..

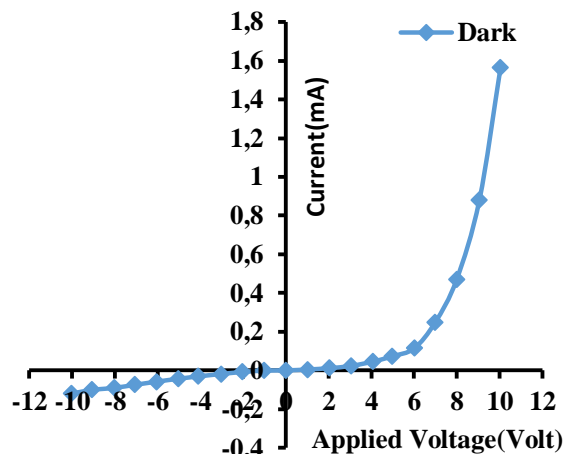


Fig. 12. I-V characteristic under forward and reverse bias of n-CdO₂/p- Si at 100 °C.

Figure 12 and 13 shows that the reversed current voltage characteristics of the device measured in dark and the photocurrent under 40 mW/cm² tungsten lamp illuminations. It can be seen that the reverse current value of a given voltage for n- CdO₂/P-Si solar cell under illumination is higher than that in the dark and it can be seen from these figures that the current value of a given voltage for heterojunction under illumination is higher than that in dark , this indicate that the light generated carrier contributing photocurrent due to the production of electron – hole as a result of the light absorption. This behavior yield useful information on the electron-hole pairs, which are effectively generated in the junction by incident photons[18].

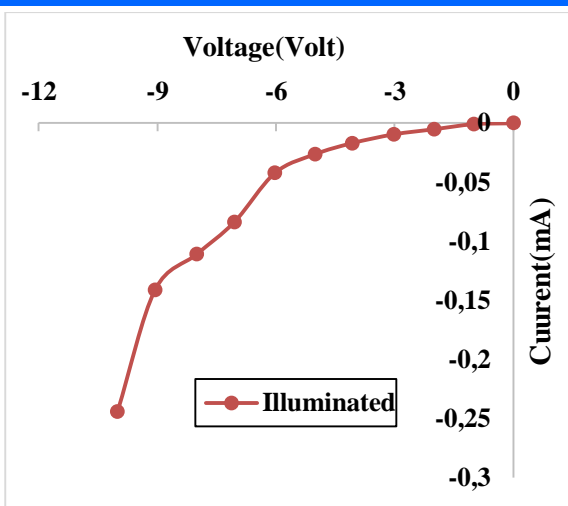


Fig.13 Illuminated (I-V) characteristic of n- CdO₂/p-Si solar cell at 100 °C

Figure. 14 shows the I-V characteristics of the solar cell under a 40 mW/cm² illumination condition .

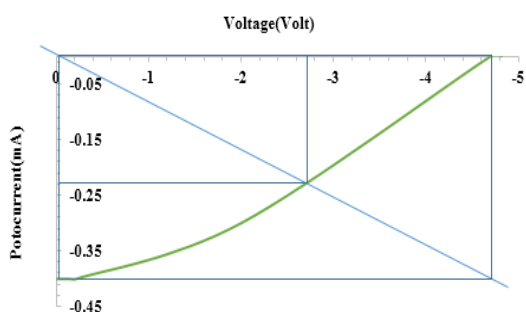


Fig14. I-V characteristics (n- CdO₂/p-Si) solar cell at 100 °C

In the present study, the n- CdO₂/P-Si solar cell has an open-circuit voltage (V_{oc}) of 4.7V, a short circuit current (I_{sc}) of 0.38mA, a maximum voltage (V_{max}) of 2.75V, and a maximum current(I_{max}) of 0.19mA.

The fill factor (FF) was calculated as follows[19].

$$FF = \frac{P_{max}}{V_{oc} \times I_{sc}} \times 100\% \quad (6)$$

FF was calculated to be 29.4%.

Cell energy conversion efficiency (η), was calculated using equation(7)

$$\eta = \frac{P_{max}}{P_{in} \times A} \times 100\% \quad (7)$$

Where P_{in} is the power input to the cell defined as the total radiant energy incident on the surface of the cell in mW/cm² , A is the surface area of the solar cell in cm² and P_{max}= V_{max}I_{max} [19].

The efficiency of the (n-CdO₂/p-Si) solar cell was 1.66% using chemical reaction

4- Conclusions

CdO₂ thin films were prepared successfully by chemical method. Bandgap value of 2.5 eV was estimated from optical characterization. X-ray diffraction (XRD) patterns approved that the CdO₂ are polycrystalline. The characteristics of n- CdO₂/p-Si shows good results which assure the suitability of using this device of solar cell applications.

References

- [1] Y. Hames and S. E. San, CdO/Cu₂O solar cells by chemical deposition, Solar Energy 77 (2004) 291-294.
- [2] F. P. Koffyberg, Diffusion of donors in semiconducting CdO, Solid State Commun. 9 (1971) 2187-2189.
- [3] F. A. Benko and F. P. Koffyberg, Quantum efficiency and optical transitions of CdO photoanodes, Solid State Commun. 57 (1986) 901 - 903.
- [4] R.L. Mishra, A.K. Sharma, S.GPrakash, Gas sensitivity and characterization of cadmium oxide semiconducting thin film deposited by spray pyrolysis technique, Digest Journal of Nanomaterials and Biostructures 4 (2009) 511-518.
- [5] K. Gurumurugan, D. Mangalraj and S.K. Narayandas, Correlations between the optical and electrical properties of CdO thin films deposited by spray pyrolysis, Thin Solid Films 251 (1994) 7-9.
- [6] O. Gomezdaza, A. Arias-Carbal Readigos, J. Campos, M. T. S. Nair, P. K. Nair, Substrate spacing and thin film yield in chemical bath deposition of semiconductor thin films, Semicond. Sci. Technol. 15(11) (2000) 1022-1029.
- [7] D.C. Renolds, D. C. Look, B. Jogai, Optically pumped ultraviolet lasing from ZnO, Solid State Comm. 99 (1996) 873-875.
- [8] L. I. Popova, S. K. Andreev, V. K. Gurorguev, E. B. Manolov, Resistance changes of SnO₂ thin films

- suitable for microelectronic gas sensors, Proceedings of the 20th international IEEE Conference on Microelectronics 2 (1995) 581-583.
- [9] K.B. Sundaram, G. K. Bhagara, Chemical vapor deposition of tin oxide films and their electrical properties, J. Phys. D: Appl. Phys. 14 (1981) 333-338.
- [10] C. H. Bhosale, A. V. Kambale, A. V. Kokate and K. Y. Rajpure, Structural, optical and electrical properties of chemically sprayed CdO thin films, Mater. Science Eng. B, 122 (2005) 67-71.
- [11] A. Salehi, M. Gholizade, Gas-sensing properties of indium-doped SnO₂ thin films with variations in indium concentration, Sensors and Actuators B: Chemical 89 (2003) 173-179.
- [12] L. Znaidi, G. J. A. A. Soler Illia, S. Beyahia, C. Sanchez and A.V. Kanaev, Oriented ZnO thin films synthesis by sol-gel process for laser application, Thin Solid Films 428 (2003) 257-262.
- [13] D.A. Lamb, S.J.C. Irvine, A temperature dependant crystal orientation transition of cadmium oxide films deposited by metal organic chemical vapour deposition, J. Cryst. Growth 332(2011) 17–20 .
- [14] E. Kashevsky, V.E. Agabekov, S.B. Kashevsky, K.A. Kekalo, E.Y. Manina, I.V. Prokhorov, V.S. Ulashchik, Study of cobalt ferrite nanosuspensions for low-frequency ferromagnetic hyperthermia Particuology 6 (2008) 322-333.
- [15] W.L. Bragg , The Structure of Magnetite and the Spinels, Nature. 95 (1915) 561-561.
- [16] B.D. Cullity, Element of X-ray Diffraction, Addison –Wesley ,Reading ,(1972) 102.
- [17] Ruby Das, , and Suman Pandey. "Comparison of optical properties of bulk and nano crystalline thin films of CdS using different precursors."International Journal of Material Science ,1(2011)35-40.
- [18] S.A.Taha,I.M.Ibrahim,N.A. Khaleafea, I-V Characteristic of CdO/PS Heterojunction, IJAIEM 3 (2014)143-148.
- [19] N.E.Makori, I. A. Amatalo, P. M. Karimi, and W. K. Njoroge, Characterization of SnSe-CdO: Sn PN Junctiono for Solar Cell Applications,International Journal of Energy Engineering 5 (2015) 1-4.